

CTC VARIATIONS THROUGH NEW WFST TOPOLOGIES

Aleksandr Laptev^{*,†}, Somshubra Majumdar^{*}, Boris Ginsburg^{*}

^{*}NVIDIA, USA

[†]ITMO University, St. Petersburg, Russia

ABSTRACT

This paper presents novel Weighted Finite-State Transducer (WFST) topologies to implement Connectionist Temporal Classification (CTC)-like algorithms for automatic speech recognition. Three new CTC variants are proposed: (1) the “compact-CTC”, in which direct transitions between units are replaced with $\langle \epsilon \rangle$ back-off transitions; (2) the “minimal-CTC”, that only adds $\langle blank \rangle$ self-loops when used in WFST-composition; and (3) “selfless-CTC”, that disallows self-loop for non-blank units. The new CTC variants have several benefits, such as reducing decoding graph size and GPU memory required for training while keeping model accuracy.

1. INTRODUCTION

Connectionist Temporal Classification (CTC) [1] is one of the most widely used algorithms to train alignment-free Automatic Speech Recognition (ASR) models. CTC loss function uses the $\langle blank \rangle$ unit to express the probability of a language unit absence in a particular timeframe. CTC allows repeated language units to indicate that the previous unit continues in the timeframe. CTC-based acoustic models can be combined with an external Language Model (LM) through a Weighted Finite-State Transducers (WFST) approach. In particular, speech decoding is performed through pruned intersection of the CTC models’ log likelihoods with a WFST graph, which represents external LM. At the decoding time, $\langle blank \rangle$ units are excluded from the recognition results, and repeated units are collapsed. However, handling of CTC repeated units complicates WFST representation. The size of CTC representation (topology or T) increases quadratically with respect to the model vocabulary. This fact makes it difficult to use word-piece tokenization dictionary with WFST decoding, or to apply sequence-discriminative criteria to CTC-like models [2].

This work studies CTC variations with respect to their WFST representations. We define CTC variation as an algorithm that allows emitting only one unit per timeframe and has a unit that serves as $\langle blank \rangle$. We consider CTC loss as forward-backward score computation of an intersection between a soft alignment graph and the acoustic outputs of a neural network. The soft alignment graph (or numerator graph) is a composition between a topology graph and a linear graph of the target unit sequence.

The paper demonstrates that by manipulating the CTC topology, it is possible to reduce the size of the decoding WFST graph and memory required to train CTC wordpiece-based models with Lattice-Free Maximum Mutual Information (LF-MMI, or just MMI) criterion [3]. It is also shown that if the CTC blank-dominant (“peaky”) behavior is endorsed by removing unit self-loops (thus prohibiting repetitive units), we can have almost the same Word Error Rate (WER) while being able to use smaller training and decoding graphs.

This work uses the k2 framework¹ [4] for the forward-backward score computation on arbitrary topologies. The code will be released as part of the NeMo toolkit² [5].

2. RELATED WORK

The first two known WFST-based CTC topologies were presented in the Eesen toolkit [6] and in [7]. These variants were suffering from training-inference topology mismatch (decoding topologies did not fully reproduce the training rules). The Eesen topology was discussed in [8], which proposed a “correct” topology and demonstrated a small WER decrease by eliminating the mismatch (see Section 2.1 for more details). Zhang et al [9] adapt chenones [10] (tied context-dependent graphemes) for CTC training, adding an extra state with $\langle blank \rangle$ for each chenone. This modification improves WER over wordpiece-based CTC models, but it limits the model’s sub-sampling factor to four. Zhao et al [11] try to decouple the $\langle blank \rangle$ property of filling the space between peaks from modeling silence to get more accurate time segments for units. Finally, [12–14] propose CTC modifications to improve language unit time alignment and reduce the peaky behavior.

2.1. Existing CTC topologies

The default CTC topology in WFST format is presented in Fig. 1 a. We refer to this as T.fst, or the correct-CTC. This is a directed complete graph with self-loops, thus for N units including $\langle blank \rangle$ there are N states and N^2 arcs. T.fst can be used for both ASR model training and WFST decoding.

The CTC topology used in Eesen toolkit [6] is presented in Fig. 1 b. We refer to this as T_{Eesen}.fst or the Eesen-CTC.

¹<https://github.com/k2-fsa/k2>

²<https://github.com/NVIDIA/NeMo>

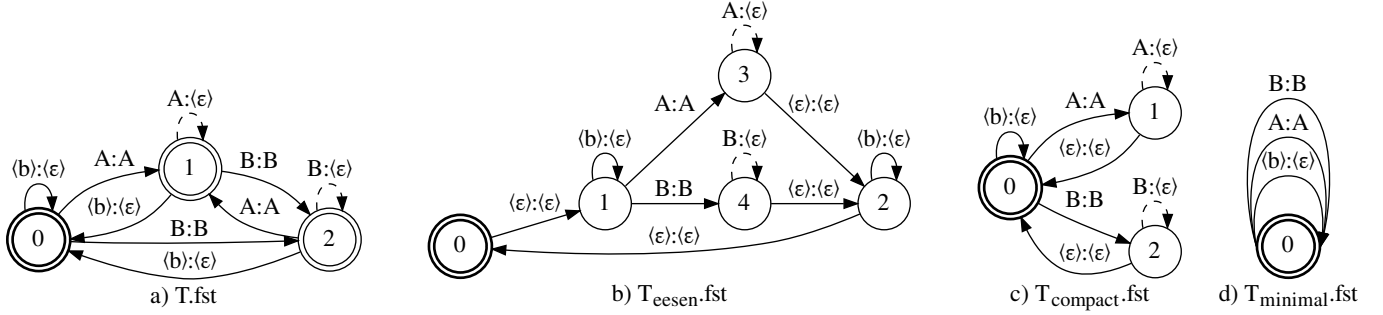


Fig. 1. Example CTC topologies for a three-unit vocabulary: $\langle blank \rangle$, A , and B . Variants: a) correct-CTC, b) Eesen-CTC, c) compact-CTC, d) minimal-CTC. $\langle b \rangle$ states for $\langle blank \rangle$. Language unit-to- $\langle \epsilon \rangle$ selfloops are indicated by dashed arrows.

This topology does not allow direct transitions between language units. It has two $\langle blank \rangle$ states which wrap all language units, and $\langle \epsilon \rangle$ -linked start state for looping them. This results in $N + 2$ states and $3N + 1$ arcs for N units. Pure $\langle \epsilon \rangle$ transitions of this graph complicate model training, since the input $\langle \epsilon \rangle$ cannot be aligned with the acoustic outputs. These transitions must be recursively traversed at each frame and represented in the resulting lattice to preserve topological order (which is required for some lattice methods, such as score computation). Thus $T_{eesen}.fst$ should only be used for WFST decoding.

3. NEW CTC TOPOLOGIES

Following the Eesen ideas, we propose a different CTC topology with pure $\langle \epsilon \rangle$ transitions, which is more compact and produces deterministic topologically sorted lattices without significant changes in training pipeline. We call it $T_{compact}.fst$ or the “compact-CTC” (Fig. 1 c). The topology has only one $\langle blank \rangle$ state, which is the destination for $\langle \epsilon \rangle$ transitions from every language unit. It has N states and $3N - 2$ arcs for N units. To be used in training, compact-CTC requires modification of either the intersection itself or the acoustic outputs to be intersected with the numerator graph. Here we consider the latter option, as it is easier to implement. An additional unit with zero probability is concatenated along the unit dimension of the acoustic output tensor. This augmented tensor is then used to fill the even timeframe slice of the final tensor, which has two times more timeframes and every odd timeframe is filled with probability 1 for each unit. The resulting tensor emulates (with 2X frame redundancy) the $\langle \epsilon \rangle$ transitions back to the $\langle blank \rangle$ state. Although this trick makes the acoustic outputs twice as long, it does not affect lattice scores significantly. Thus, training with compact-CTC is expected to produce models performing close to the $T.fst$ baseline.

$T_{compact}.fst$ can be simplified even more if we remove all language unit-to- $\langle \epsilon \rangle$ self-loops and collapse the $\langle \epsilon \rangle$ transitions. The variant that we define as $T_{minimal}.fst$ topology or the “minimal-CTC” is presented in Fig. 1 d. It has only one state and does only one non-trivial transduction from $\langle blank \rangle$ to $\langle \epsilon \rangle$, resulting in N arcs for N units. $T_{minimal}.fst$ can be used for both ASR model training and WFST decoding.

The idea of removing language unit-to- $\langle \epsilon \rangle$ self-loops can also be applied to any of the aforementioned topologies except $T_{minimal}.fst$, where there are no such self-loops by design. We call this variation “selfless-CTC”. Variants of selfless-CTC can be obtained from Fig. 1 by removing dashed transitions. Note that while selfless $T_{compact}.fst$ and $T_{minimal}.fst$ are used differently in training ($T_{minimal}.fst$ does not require manipulations performed for $T_{compact}.fst$), removing self-loops from $T_{compact}.fst$ makes it almost identical to $T_{minimal}.fst$ from the Kaldi [15] WFST decoding perspective ($\langle \epsilon \rangle$ transitions are processed in a breadth-first manner in a single decoding iteration; this leads to almost identical unit pools when using graphs differing only in $\langle \epsilon \rangle$ transitions). Decoding with regular $T_{compact}.fst$ is also expected to be identical to using $T_{eesen}.fst$, thus the topology that results in a smaller decoding graph should be used.

4. EXPERIMENTS

4.1. Experimental setup

We used NeMo toolkit for ASR training, k2 framework to compute loss functions on arbitrary topologies, and cuSpeech toolkit (to be published) for GPU WFST decoding [16].

We considered three ASR models: Citrinet-384, Citrinet-1024 [17], and Conformer-L [18]. Experiments were performed with the 3-way speed-perturbed LibriSpeech [19], and the 4-gram word-level LM, provided with the dataset. The following settings are used by default unless otherwise noted:

- The default ASR model is Citrinet-384 with context scaling factor $\gamma = 0.25$, trained for 400 epochs on 32 V100 GPUs, and with 256 Byte-Pair Encoding (BPE) wordpiece vocabulary. CTC models were trained with batch 32 per GPU.
- MMI models were trained with bi-gram unit-level LMs without backoff probabilities. Decoding graphs for MMI models include the unit-level LM used in training, that is composed with the topology graph. MMI models were first trained with batch 16 per GPU and gradient accumulation 2 for 4 epochs, then with batch 32 for the rest of the training (see Section 4.4).
- WER results were obtained with WFST decoding on a graph constructed with the same topology used to train a particular model.

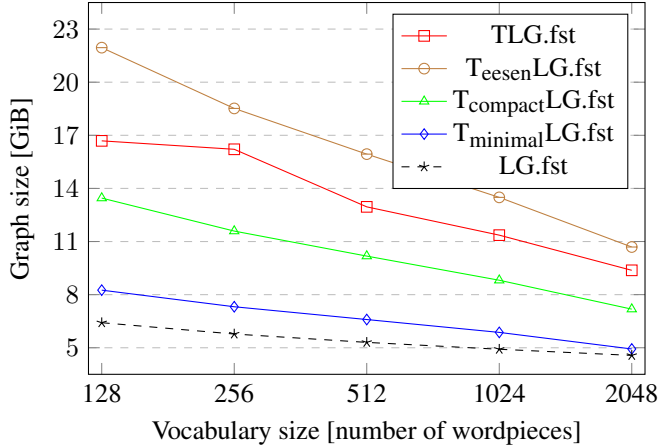


Fig. 2. Decoding graph sizes with the considered topologies.

4.2. Preliminary study

A decoding graph consists of a topology graph, a lexicon graph (*L.fst*) that maps vocabulary unit sequences to words, and a word-level LM graph (*G.fst*, or grammar) composed together. Fig. 2 shows a comparison of different decoding graph sizes for different vocabulary sizes. The decoding graph TLG.fst sets the baseline, and the language graph LG.fst serves as the lower bound of the size a decoding graph can have. T_{eesen}LG.fst has larger sizes than the baseline while using T_{compact}LG.fst reduces memory consumption by a quarter. T_{minimal}.fst gives the least topology overhead because it introduces only the *<blank>* self-loops when composed with LG.fst. Based on this data and the above discussion on *<ε>* transitions, we exclude T_{eesen}LG.fst and selfless-T_{compact}LG.fst from consideration. At the same time, selfless-TLG.fst is of interest because it cannot be fully emulated using any other topology, and its size is smaller than that of the baseline TLG.fst.

The initial experiments were to evaluate the CTC ability to operate effectively with the alternative topologies that can be used in training. They are: T.fst and T_{compact}.fst with or without self-loops, and T_{minimal}.fst. The first part of Table 1 contains WER results of purely CTC-trained models with different topologies. While with CTC loss all the proposed variations demonstrated a significant accuracy drop against

Table 1. CTC-trained vs MMI-trained variations, WER [%]

Loss	CTC variants	Dev		Test	
		clean	other	clean	other
CTC	correct	2.57	6.82	2.91	6.98
	correct selfless	3.52	9.10	3.72	9.61
	compact	na	na	na	na
	compact selfless	3.69	9.65	3.95	9.89
	minimal	3.74	9.52	3.99	10.07
MMI	correct	2.65	6.64	2.91	6.82
	correct selfless	2.66	6.80	2.96	6.94
	compact	2.66	6.62	2.98	6.83
	compact selfless	2.80	7.14	3.14	7.45
	minimal	2.85	7.14	3.01	7.36

Table 2. Citrinet-1024, variants with self-loops, WER [%]

Loss	Decode	Dev		Test	
		clean	other	clean	other
CTC	greedy	2.38	6.00	2.57	5.87
	TLG.fst	2.12	4.83	2.40	5.12
	T _{compact} LG.fst	2.12	4.83	2.39	5.13
MMI	greedy	2.16	5.55	2.36	5.35
	TLG.fst	2.14	4.78	2.40	4.89
	T _{compact} LG.fst	2.14	4.78	2.39	4.89
MMI compact	greedy	2.27	5.34	2.31	5.32
	TLG.fst	2.23	4.55	2.43	4.93
	T _{compact} LG.fst	2.22	4.50	2.41	4.93

correct-CTC as a baseline (furthermore, compact-CTC did not converge), with MMI loss all the variations demonstrate close results (the second part of Table 1). In the rest of the paper, we explore topologies with MMI loss only.

4.3. The MMI models with different CTC variants

We considered two ASR models: Citrinet-1024 and Conformer-L, trained for 1k epochs. WER is measured with five decoding approaches: greedy (usual argmax for CTC models and “argmax of pairs” – intersection with the bi-gram training LM for MMI models), and WFST decoding with TLG.fst, selfless-TLG.fst, T_{compact}LG.fst, and T_{minimal}LG.fst. Only applicable decoding approaches are demonstrated for each model. In Tables 2–5 values in Loss column state as follows: “CTC” for a CTC-trained model with T.fst topology, “MMI” for an MMI-trained model with T.fst, “MMI compact” for T_{compact}.fst, and “MMI minimal” for T_{minimal}.fst.

Tables 2 and 3 demonstrate results for Citrinet-1024 and variants with- and without self-loops, respectively. The MMI models, while being generally better, enjoyed lesser accuracy improvement than the CTC model from decoding with WFST graph versus greedy mode. Decoding with T_{compact}LG.fst is preferred over TLG.fst because it performed approximately the same as TLG.fst while requiring less memory space. Compact-CTC and selfless-CTC models performed close to the correct-CTC. Moreover, WER increase due to topology mismatch when using T_{minimal}LG.fst with the correct-selfless-CTC did not exceed 0.2%. This might be a reasonable tradeoff because the size of T_{minimal}LG.fst is nearly 2 times smaller than TLG.fst. Compact-selfless-CTC and minimal-

Table 3. Citrinet-1024, selfless-CTC, WER [%]

Loss	Decode	Dev		Test	
		clean	other	clean	other
MMI	greedy	2.22	5.42	2.43	5.32
	TLG.fst	2.11	4.64	2.43	4.91
	T _{minimal} LG.fst	2.23	4.76	2.53	5.07
MMI compact	greedy	2.39	6.22	2.64	6.13
	T _{minimal} LG.fst	2.22	5.16	2.56	5.33
MMI minimal	greedy	2.41	6.53	2.71	6.25
	T _{minimal} LG.fst	2.27	5.11	2.64	5.36

Table 4. Conformer-L, variants with self-loops, WER [%]

Loss	Decode	Dev		Test	
		clean	other	clean	other
CTC	greedy	2.52	6.50	2.94	6.65
	TLG.fst	2.27	5.11	2.68	5.35
	T _{compact} LG.fst	2.28	5.10	2.67	5.35
MMI	greedy	2.58	6.35	2.69	6.48
	TLG.fst	2.32	5.20	2.61	5.58
	T _{compact} LG.fst	2.32	5.20	2.61	5.56
MMI compact	greedy	2.42	6.39	2.62	6.51
	TLG.fst	2.23	5.10	2.55	5.58
	T _{compact} LG.fst	2.24	5.09	2.55	5.56

CTC performed worse than the CTC baseline.

In contrast to Citrinet-1024, Conformer-L (trained with 128 BPE wordpieces, and with batch 16 on 128 V100 GPUs) did not benefit much from using MMI (Tables 4 and 5). Only compact-selfless-CTC slightly outperformed the CTC baseline. Other decoding-related observations are consistent with those obtained earlier for Citrinet-1024.

4.4. The effect of context and vocabulary sizes on models with different topologies.

Since the best models for our Conformer (unlimited context) and Citrinet ($\gamma = 0.25$, 11 frames of context) belong to different self-loop variants, we compared two Citrinets with different context sizes ($\gamma = 0.25$ and $\gamma = 1.0$). Compact-selfless-CTC and minimal-CTC models are excluded from this consideration as less effective than the other variants. According to Table 6, variants with self-loops performed better than without for the short context. However, for the longer context these variants show some WER increase, while selfless-CTC improved the accuracy and delivered the best result overall. This finding is consistent with the Conformer results in Section 4.3. Removing self-loops from the CTC topology may be beneficial for ASR models with long contexts.

LF-MMI models are usually trained on chunks of 1 to 1.5 seconds in Kaldi and PyChain [20], while we trained our models on whole utterances (since there are no reference alignment for CTC-MMI models), which are 10 to 15 times longer. In addition, to train MMI models with BPE units, we had to reduce batch (and increase gradient accumulation accordingly) for a certain number of initial epochs, because

Table 5. Conformer-L, selfless-CTC, WER [%]

Loss	Decode	Dev		Test	
		clean	other	clean	other
MMI	greedy	2.56	6.49	2.80	6.48
	TLG.fst	2.23	4.99	2.54	5.33
	T _{minimal} LG.fst	2.34	5.11	2.68	5.50
MMI compact	greedy	3.09	8.24	3.39	7.99
	T _{minimal} LG.fst	2.50	5.91	2.82	6.01
MMI minimal	greedy	3.24	8.64	3.42	8.50
	T _{minimal} LG.fst	2.55	6.17	2.80	6.28

Table 6. Variations against different context sizes, WER [%]

Gamma	CTC variants	Dev		Test	
		clean	other	clean	other
0.25	correct	2.65	6.64	2.91	6.82
	correct selfless	2.66	6.80	2.96	6.94
	compact	2.66	6.62	2.98	6.83
1.0	correct	2.58	6.61	2.99	6.86
	correct selfless	2.60	6.43	2.86	6.64
	compact	2.68	6.81	3.06	7.01

the log-probabilities are uniformly distributed at the start of the training. All this leads to a sharp increase in the denominator lattice size and causes Out Of Memory (OOM) errors. Table 7 demonstrates the maximum initial batch that does not cause OOM for models with different topologies relative to the BPE vocabulary size. The most memory efficient topology is T_{minimal}.fst, and T_{compact}.fst provides a steady memory consumption reduction against T.fst.

Table 7. Maximum initial batch.

Voc. size	CTC variants				
	correct	correct selfless	compact	compact selfless	minimal
256	16	16	32	32	32
512	8	4	16	16	16
1024	4	4	8	8	8
2048	1	1	2	2	4

5. CONCLUSION

This paper presented a thorough study of novel WFST graph representations (topologies) for CTC-like algorithms for training and inference of ASR models. We analyzed the existing CTC topologies and proposed three new CTC-like variants. “Compact-CTC” topology and corresponding traversal algorithm replaces direct transitions between units with $\langle\epsilon\rangle$ back-off transitions. WFST graph of this variant is fully compatible with the classic (correct) CTC and provides the same decoding accuracy. “Minimal-CTC” topology only adds $\langle\text{blank}\rangle$ -to- $\langle\epsilon\rangle$ self-loops when used in WFST-composition. The decoding graph for this variant has the minimal topology-induced overhead, and its size is half that of the base graph. “Selfless-CTC” variation disallows language unit-to- $\langle\epsilon\rangle$ self-loops for any CTC variant except minimal-CTC. Any selfless-CTC variant is compatible with the minimal-CTC graph at decoding. Also, selfless-CTC for the correct topology can reduce WER for wide context window models. The proposed topologies produce smaller decoding graphs and require less GPU memory when used in LF-MMI loss.

6. ACKNOWLEDGEMENTS

We would like to thank V. Noroozi, V. Lavrukhin, D. Galvez, and the k2-FSA team for their help and discussions.

7. REFERENCES

- [1] A. Graves, S. Fernández, F. Gomez, and J. Schmidhuber, “Connectionist temporal classification: labelling unsegmented sequence data with recurrent neural networks,” in *ICML*, 2006.
- [2] H. Zheng, W. Peng, Z. Ou, and J. Zhang, “Advancing CTC-CRF based end-to-end speech recognition with wordpieces and conformers,” *arXiv:2107.03007*, 2021.
- [3] D. Povey, V. Peddinti, D. Galvez, P. Ghahremani, V. Manohar, X. Na, Y. Wang, and S. Khudanpur, “Purely Sequence-Trained Neural Networks for ASR Based on Lattice-Free MMI,” in *Interspeech*, 2016.
- [4] D. Povey, P. Želasko, and S. Khudanpur, “Speech recognition with next-generation kaldi (k2, lhotse, icefall),” *Interspeech: tutorials*, 2021.
- [5] O. Kuchaiev, J. Li, H. Nguyen, O. Hrinchuk, R. Leary, B. Ginsburg, S. Krizan, S. Beliaev, V. Lavrukhin, J. Cook, et al., “NeMo: a toolkit for building AI applications using neural modules,” *arXiv:1909.09577*, 2019.
- [6] Y. Miao, M. Gowayyed, and F. Metze, “EESN: End-to-end speech recognition using deep rnn models and wfst-based decoding,” in *ASRU*, 2015.
- [7] H. Sak, A. Senior, K. Rao, O. İrsoy, A. Graves, F. Beaufays, and J. Schalkwyk, “Learning acoustic frame labeling for speech recognition with recurrent neural networks,” in *ICASSP*, 2015.
- [8] H. Xiang and Zh. Ou, “CRF-based single-stage acoustic modeling with CTC topology,” in *ICASSP*, 2019.
- [9] F. Zhang, Y. Wang, X. Zhang, C. Liu, Y. Saraf, and G. Zweig, “Faster, Simpler and More Accurate Hybrid ASR Systems Using Wordpieces,” in *Interspeech*, 2020.
- [10] D. Le, X. Zhang, W. Zheng, Ch. Fügen, G. Zweig, and M. L. Seltzer, “From senones to chenones: Tied context-dependent graphemes for hybrid speech recognition,” in *ASRU*, 2019.
- [11] T. Zhao, “A novel topology for end-to-end temporal classification and segmentation with recurrent neural network,” *arXiv:1912.04784*, 2019.
- [12] H. Liu, Sh. Jin, and Ch. Zhang, “Connectionist temporal classification with maximum entropy regularization,” in *NeuRIPS*, 2018.
- [13] L. Hongzhu and W. Weiqiang, “Reinterpreting CTC training as iterative fitting,” *Pattern Recognition*, 2020.
- [14] A. Zeyer, R. Schlüter, and H. Ney, “Why does CTC result in peaky behavior?,” *arXiv:2105.14849*, 2021.
- [15] D. Povey, A. Ghoshal, G. Boulianne, L. Burget, O. Glembek, N. Goel, M. Hannemann, P. Motlicek, Y. Qian, P. Schwarz, J. Silovsky, G. Stemmer, and K. Vesely, “The Kaldi speech recognition toolkit,” in *ASRU*, 2011.
- [16] H. Braun, J. Luitjens, R. Leary, T. Kaldewey, and D. Povey, “GPU-accelerated Viterbi exact lattice decoder for batched online and offline speech recognition,” in *ICASSP*, 2020.
- [17] S. Majumdar, J. Balam, O. Hrinchuk, V. Lavrukhin, V. Noroozi, and B. Ginsburg, “Citrinet: Closing the gap between non-autoregressive and autoregressive end-to-end models for automatic speech recognition,” *arXiv:2104.01721*, 2021.
- [18] A. Gulati, J. Qin, C.-C. Chiu, N. Parmar, Y. Zhang, J. Yu, W. Han, S. Wang, Z. Zhang, Y. Wu, and R. Pang, “Conformer: Convolution-augmented Transformer for Speech Recognition,” in *Interspeech*, 2020.
- [19] V. Panayotov, G. Chen, D. Povey, and S. Khudanpur, “LibriSpeech: an ASR corpus based on public domain audio books,” in *ICASSP*, 2015.
- [20] Y. Shao, Y. Wang, D. Povey, and S. Khudanpur, “PyChain: A Fully Parallelized PyTorch Implementation of LF-MMI for End-to-End ASR,” in *Interspeech*, 2020.